ESTIMATION OF VISUAL EVOKED POTENTIAL LATENCIES USING KARHUNEN LOEVE TRANSFORM METHOD

Mohd Zuki Yusoff

Electrical & Electronic Engineering Department, University Teknologi PETRONAS
Bandar Seri Iskandar, 31750 Tronoh, Perak, MALAYSIA
phone: + (605) 368 7807, fax: + (605) 365 7443, email: mzuki_yusoff@petronas.com.my
web: http://www.utp.edu.my

ABSTRACT

Estimating a signal which is buried inside colored noise is challenging since significant amount of the noise frequencies with considerable or higher power reside in the same band as that of the desired waveform. In this paper, an optimization- and Karhunen-Loeve Transform (KLT)-based approach has been investigated and tested to estimate the latencies of single-trial visual evoked potentials (VEPs) which are highly corrupted by colored electroencephalogram (EEG) noise. The normal voltage level for a VEP is around 10 µV and the background EEG is in the proximity of 100 µV, producing a signal-to-noise ratio (SNR) in the range of -10 dB. The studied method devices an explicit pre-whitening scheme aimed at producing a symmetric basis matrix, which eventually generates a unitary eigenvector matrix that simultaneously diagonalizes both the wanted signal and noise correlation matrices. The absolute diagonalization ensures full decorrelation of the observed signal, and permits the segregation of the transformed signal space into the "signal plus noise subspace" and "noise only subspace." The performance of the KLT-based method in estimating VEP latencies has been assessed using comprehensively and realistically simulated data at SNR ranging from 0 to -10 dB, and real patient data gathered in a hospital. The technique produces reasonably high success rates, high accuracies and precisions, and narrow standard deviations in both experiments.

Keywords: *Karhunen-Loeve transform, eigenvalue decomposition, subspace methods, time-domain estimator, visual evoked potentials.*

1. INTRODUCTION

Visual evoked potentials (VEPs) are special types of elecroencephalogram (EEG) signals generated by the human brain when a specific visual stimulation is applied to the eye (left or right) of the subject under study. In a hospital, a visual evoked potential test is used as an **objective test** to assess the conduction of the human visual pathway from the retina to the brain's occipital cortex. Usually, the latency of the robust and positive going P100 component is used by doctors to determine the normality/abnormality of a subject's optical pathway. The ideal P100 values are 100 ms; the borderline P100's value for a normal subject is 115 ms. This means, subjects with defective visual pathways will register prolonged P100 latencies greater than 115 ms (e.g., at 120 ms, 130 ms, etc.). Conventionally, VEPs are extracted from the spontaneous brain activity by collecting a series of time-locked electroencephalogram (EEG) epochs and performing multi-trial ensemble averaging (EA) on these samples to improve the SNR. Alternatively, a VEP estimation scheme based on a single VEP trial can be developed to reduce VEP recording time, minimize fatigue on subjects, and promote consistencies in the outcome of the VEP latencies.

The focus of this study is to correctly estimate VEP latencies, instead of VEP amplitudes; clinicians are more interested in the VEP latencies as opposed to the VEP amplitudes, as far as the VEP test is concerned. The VEP extraction method presented here is inspired by work from a speech enhancement area, originally proposed by Ephraim and Van Trees [1] for white noise elimination, and further extended by Rezayee and Gazor [2], and Lev-Ari and Ephraim [3] to deal with colored noise.

Moreover, this paper is an extension of our signal subspace work reported in [4]. In [4], we applied the constrained optimization concept suggested by [1] and adapted the estimator enhanced by [2] to estimate the P100 components from EEG background, without using a pre-whitening stage. In this paper, we still utilize the minimization procedure in [1] and now adapt [3] to extract VEPs and estimate the associated P100 latencies. The application of [3] results in better VEP estimation performance in comparison to the application of [2]. This is because the technique in [3] permits full diagonalization of signal and noise covariance matrices, as opposed to that in [2] which only approximately diagonalizes the two matrices.

2. MODEL DEVELOPMENT

2.1 VEP Model

It is assumed that a VEP is actually a “known" waveform which can be artificially produced. The created VEP will then be added to much higher power “colored noise” that represents EEG and other background noise. Thus, the following model is defined.

$$\boldsymbol{y} = \boldsymbol{x} + \boldsymbol{n} \tag{1}$$

where, $\boldsymbol{y}$ is the M-dimensional vector of the corrupted (noisy) VEP signal; $\boldsymbol{x}$ is the M-dimensional vector of the original (clean) VEP signal; $\boldsymbol{n}$ is the M-dimensional vector of the additive EEG noise which is assumed to be uncorrelated with $\boldsymbol{x}$. Further, $\boldsymbol{H}$ is defined as the M x M-dimensional matrix of the VEP time-domain constrained linear estimator.

Next, $\hat{\boldsymbol{x}}$ is defined as the M-dimensional vector of the estimated VEP signal. The estimated VEP signal $\hat{\boldsymbol{x}}$ is related to $\boldsymbol{H}$ and $\boldsymbol{y}$ in the following way:

$$\hat{\boldsymbol{x}} = \boldsymbol{H} \cdot \boldsymbol{y} \tag{2}$$

The estimated VEP signal $\hat{\boldsymbol{x}}$ will never be exactly equal to the original VEP signal $\boldsymbol{x}$; the error signal $\boldsymbol{\varepsilon}$ defined by [1] is written as:

$$\begin{aligned} \boldsymbol{\varepsilon} &= \hat{\boldsymbol{x}} - \boldsymbol{x} = \boldsymbol{H}\boldsymbol{y} - \boldsymbol{x} = (\boldsymbol{H} - \boldsymbol{I})\boldsymbol{x} + \boldsymbol{H}\boldsymbol{n} \\ &= \boldsymbol{\varepsilon}_x + \boldsymbol{\varepsilon}_n \quad \text{where } \boldsymbol{\varepsilon}_x = (\boldsymbol{H} - \boldsymbol{I})\boldsymbol{x}, \quad \boldsymbol{\varepsilon}_n = \boldsymbol{H}\boldsymbol{n} \end{aligned} \tag{3}$$

The $\boldsymbol{\varepsilon}_x$ represents the VEP distortion and $\boldsymbol{\varepsilon}_n$ represents the residual noise. If the VEP signal covariance matrix $\boldsymbol{R}_x$ is known, then the energies of the signal distortion can be written as

$$\bar{\boldsymbol{\varepsilon}}_x^2 = \mathrm{tr}\left(E\left\{\boldsymbol{\varepsilon}_x \boldsymbol{\varepsilon}_x^T\right\}\right) = \mathrm{tr}\left((\boldsymbol{H} - \boldsymbol{I})\boldsymbol{R}_x(\boldsymbol{H} - \boldsymbol{I})^T\right) \tag{4}$$

Similarly, if the EEG noise covariance matrix $\boldsymbol{R}_n$ is known, the energies of the residual noise can be expressed as

$$\bar{\boldsymbol{\varepsilon}}_n^2 = \mathrm{tr}\left(E\left\{\boldsymbol{\varepsilon}_n \boldsymbol{\varepsilon}_n^T\right\}\right) = \mathrm{tr}\left(\boldsymbol{H}\boldsymbol{R}_n\boldsymbol{H}^T\right) \tag{5}$$

Both energies in (4) and (5) lead to the total residual energies given as

$$\bar{\boldsymbol{\varepsilon}}^2 = \bar{\boldsymbol{\varepsilon}}_x^2 + \bar{\boldsymbol{\varepsilon}}_n^2 \tag{6}$$

The EEG noise covariance matrix $\boldsymbol{R}_n$ can be obtained from the pre-stimulation EEG samples, during which the VEP signals are absent. If the VEP and EEG noise are independent, the following relationships can be established:

$$\boldsymbol{R}_y = \boldsymbol{R}_x + \boldsymbol{R}_n \tag{7}$$

where, $\boldsymbol{R}_y$ is the covariance matrix of the corrupted VEP. Using (7), we can approximate $\boldsymbol{R}_x$ by subtracting $\boldsymbol{R}_n$ from $\boldsymbol{R}_y$. The aim is to minimize the unwanted energies in (6) so that the generated error is minimal. A difficulty arises since lowering noise energies means increasing the distortion energies, and vice versa. Therefore, a proper balance needs to be determined so that the noise residues can be reasonably reduced without introducing significant distortion to the processed signal. The excessive amount of the residual noise prohibits the discrimination between the desired VEP peak (i.e., the P100) and the noise peaks itself, even if the desired signal is successfully extracted. On the other hand, the excessive distortion means the desired VEP peak may have shifted either to the left or right of its original position, resulting in an inaccurate measurement of the VEP latency.

2.2 Estimator Optimization

An optimal time domain constrained linear estimator $\boldsymbol{H}$ that minimizes the VEP signal distortion and maintains the residual noise within a permissible level, is mathematically formulated by [1] as

$$\boldsymbol{H}_{opt} = \min_{\boldsymbol{H}} \ \bar{\boldsymbol{\varepsilon}}_x^2 \ \text{ subject to} : \bar{\boldsymbol{\varepsilon}}_n^2 \leq M\sigma^2 \tag{8}$$

where M is the dimension of the noisy vector space and σ^2 is a positive constant noise threshold level. The σ^2 in (8) dictates the amount of the residual noise allowed to remain in the linear estimator. Next, the Lagrangian function in association with the "Kuhn-Tucker necessary conditions for constrained minimization" [1] are applied to (8) to obtain $\boldsymbol{H}_{opt}$. The formed Lagrangian function can be expressed as

$$\boldsymbol{L}(\boldsymbol{H}, \mu) = \bar{\boldsymbol{\varepsilon}}_x^2 + \mu(\bar{\boldsymbol{\varepsilon}}_n^2 - M\sigma^2) \tag{9}$$

where μ is the Lagrange multiplier. It follows that the filter matrix $\boldsymbol{H}$ is a stationary feasible point if it satisfies the following gradient equation $\nabla_H \boldsymbol{L}(\boldsymbol{H}, \mu) = 0$:

$$\frac{\partial \boldsymbol{L}(\boldsymbol{H}, \mu)}{\partial \boldsymbol{H}} = \frac{\partial}{\partial \boldsymbol{H}}[\bar{\boldsymbol{\varepsilon}}_x^2 + \mu(\bar{\boldsymbol{\varepsilon}}_n^2 - M\sigma^2)] = 0 \tag{10}$$

Subsequently, the gradient equation in (10) can be solved to yield the following $\boldsymbol{H}$.

$$\boldsymbol{H} = \boldsymbol{R}_x(\boldsymbol{R}_x + \mu\boldsymbol{R}_n)^{-1} \tag{11}$$

The filter matrix $\boldsymbol{H}$ stated in (11) functions as a fixed filter, which performs well to estimate the VEP at a relatively high SNR. As the SNR degrades, it is desirable if $\boldsymbol{H}$ can be adjusted and manipulated accordingly to minimize the noise residues while keeping the signal distortion at an acceptable level.

2.3 Generic Subspace Approach

With reference to (11), eigenvalue decomposition is to be performed on $\boldsymbol{R}_x$ and $\boldsymbol{R}_n$. By assuming that $\boldsymbol{R}_x = \boldsymbol{U}\boldsymbol{\Delta}_x\boldsymbol{U}^T$ and $\boldsymbol{R}_n = \boldsymbol{U}\boldsymbol{\Delta}_n\boldsymbol{U}^T$ exist, we rewrite (11) as

$$\boldsymbol{H}_{opt} = \boldsymbol{U}\boldsymbol{\Delta}_x(\boldsymbol{\Delta}_x + \mu\boldsymbol{\Delta}_n)^{-1}\boldsymbol{U}^T \tag{12}$$

where, $\boldsymbol{H}_{opt}$ denotes an optimal estimator; $\boldsymbol{U}$ is the unitary eigenvector matrix produced from a symmetric basis matrix $\boldsymbol{\Sigma}$ which is to be computed from the proper combinations of $\boldsymbol{R}_x$ and $\boldsymbol{R}_n$ terms; $\boldsymbol{\Delta}_x$ is the diagonal eigenvalue matrix of $\boldsymbol{R}_x$; $\boldsymbol{\Delta}_n$ is the diagonal eigenvalue matrix of $\boldsymbol{R}_n$; μ is the Lagrange multiplier which has to be set to a proper value. The higher value of μ eliminates more noise residues at the expense of higher distortion in the recovered VEP.

Theoretically, the linear estimator in (12) functions optimally if the unitary eigenvector matrix $\boldsymbol{U}$ derived from $\boldsymbol{\Sigma}$ is able to simultaneously diagonalize both $\boldsymbol{R}_x$ and $\boldsymbol{R}_n$. The full diagonalization of their eigenvalues can be obtained if and only if $\boldsymbol{R}_x$ and $\boldsymbol{R}_n$ multiplication is commutative (i.e., $\boldsymbol{R}_x\boldsymbol{R}_n = \boldsymbol{R}_n\boldsymbol{R}_x$). In reality, complete diagonalization (i.e., without pre-whitening) is not possible since their multiplication is non-commutative.

2.4 Karhunen-Loeve Transform Method Based on the Explicit Prewhitening of the Correlation Matrix of the Desired Signal

Next, we employ the basis matrix $\boldsymbol{R} = \boldsymbol{R}_n^{-1/2}\boldsymbol{R}_x\boldsymbol{R}_n^{-1/2}$ from [3] to create a unitary eigenvector matrix $\boldsymbol{V}$ that indirectly, simultaneously and fully diagonalizes both $\boldsymbol{R}_x$ and $\boldsymbol{R}_n$. To make use of $\boldsymbol{R}$, (11) will need to be further manipulated to yield the following:

$$\begin{aligned} \boldsymbol{H} &= \boldsymbol{I}_1\boldsymbol{R}_x\boldsymbol{I}_2(\boldsymbol{I}_1\boldsymbol{R}_x\boldsymbol{I}_2 + \mu\boldsymbol{I}_1\boldsymbol{R}_n\boldsymbol{I}_2)^{-1}, \boldsymbol{I}_1 = \boldsymbol{I}_2^{-1} = \boldsymbol{R}_n^{1/2}\boldsymbol{R}_n^{-1/2} \\ &= \boldsymbol{R}_n^{1/2}\boldsymbol{R}(\boldsymbol{R}+\mu\boldsymbol{I})^{-1}\boldsymbol{R}_n^{-1/2}, \text{ where } \boldsymbol{R} = \boldsymbol{R}_n^{-1/2}\boldsymbol{R}_x\boldsymbol{R}_n^{-1/2} \end{aligned} \tag{13}$$

The eigendecomposition operation of the symmetric basis matrix $\boldsymbol{R} = \boldsymbol{R}_n^{-1/2}\boldsymbol{R}_x\boldsymbol{R}_n^{-1/2}$ leads to the following:

$$\boldsymbol{RV} = \boldsymbol{V\Lambda} \tag{14}$$

$$\boldsymbol{V}^T\boldsymbol{RV} = \boldsymbol{\Lambda} \quad \leftrightarrow \quad \boldsymbol{R} = \boldsymbol{V}^{-T}\boldsymbol{\Lambda}\boldsymbol{V}^{-1} = \boldsymbol{V\Lambda V}^T \tag{15}$$

where $\boldsymbol{\Lambda}$ and $\boldsymbol{V}$ are, respectively, the eigenvalue and unitary eigenvector matrices of $\boldsymbol{R}$. It is to be noted that $\boldsymbol{V}^{-T} = \boldsymbol{V}$ and $\boldsymbol{V}^{-1} = \boldsymbol{V}^T$ for unitary $\boldsymbol{V}$. By putting $\boldsymbol{R}$ in (15) into (13), the KLTM-based $\boldsymbol{H}$ can be written as

$$\begin{aligned} \boldsymbol{H} &= \boldsymbol{R}_n^{1/2}\boldsymbol{V\Lambda V}^T(\boldsymbol{V\Lambda V}^T + \mu\boldsymbol{I})^{-1}\boldsymbol{R}_n^{-1/2} \\ &= \boldsymbol{R}_n^{1/2}\boldsymbol{VGV}^T\boldsymbol{R}_n^{-1/2}, \text{ where } \boldsymbol{G} = \boldsymbol{\Lambda}(\boldsymbol{\Lambda}+\mu\boldsymbol{I})^{-1} \end{aligned} \tag{16}$$

where $\boldsymbol{G}$ is known as the gain matrix. Based on (2) and (16), the estimated VEP can be expressed as

$$\begin{aligned} \hat{\boldsymbol{x}}_{KLTM} &= \boldsymbol{H}\cdot\boldsymbol{y} = \boldsymbol{R}_n^{1/2}\boldsymbol{V\Lambda}(\boldsymbol{\Lambda}+\mu\boldsymbol{I})^{-1}\boldsymbol{V}^T\boldsymbol{R}_n^{-1/2}\cdot\boldsymbol{y} \\ &= \boldsymbol{R}_n^{1/2}\boldsymbol{VGV}^T\boldsymbol{R}_n^{-1/2}\cdot\boldsymbol{y},\ \boldsymbol{G} = \boldsymbol{\Lambda}(\boldsymbol{\Lambda}+\mu\boldsymbol{I})^{-1} \end{aligned} \tag{17}$$

The corrupted VEP $\boldsymbol{y}$ in (17) is explicitly pre-whitened by $\boldsymbol{R}_n^{-1/2}$. Afterwards, the whitened signal is decorrelated by the KLT matrix $\boldsymbol{V}^T$. Then, the transformed signal is modified by a signal subspace gain matrix $\boldsymbol{G}$. Next, the modified signal is retransformed back into the original form by the inverse KLT matrix $\boldsymbol{V}$. The retransformed signal is further de-whitened by $\boldsymbol{R}_n^{1/2}$ to obtain the desired VEP signal.

2.5 Algorithm Implementation

The proposed approach can be formulated in the following eight steps. For each VEP trial:

Step 1: Compute the covariance matrix of the noisy signal $\boldsymbol{R}_y$ which can be directly obtained from the observed (corrupted) signal.
Step 2: Estimate the covariance matrix of the noise $\boldsymbol{R}_n$ which can be obtained from the pre-stimulation EEG, during which the VEP sample is absent.
Step 3: Approximate the covariance matrix of the desired signal $\boldsymbol{R}_x$, by using $\boldsymbol{R}_x = \boldsymbol{R}_y - \boldsymbol{R}_n$.
Step 4: Perform the eigendecomposition operation on the basis matrix $\boldsymbol{R} = \boldsymbol{R}_n^{-1/2}\boldsymbol{R}_x\boldsymbol{R}_n^{-1/2}$ and extract the resulting unitary eigenvector and eigenvalue matrices $\boldsymbol{V}$ and $\boldsymbol{\Lambda}$, respectively.
Step 5: Assuming that λ_k series represented by $\lambda_1 > \lambda_2 > \lambda_3 \ldots \lambda_M$ are the diagonal elements of $\boldsymbol{\Lambda}$ sequenced in descending order, approximate the dimension L of the VEP signal subspace by counting the number of non-zero elements of $\boldsymbol{\Lambda}$.

$$L = \arg\{\max_{1\le k\le M} \lambda_k > 0\} \tag{18}$$

Step 6: Compute the gain vector of the KLTM estimator as follows:

$$q(i) = \lambda_X(i)/(\lambda_X(i)+\mu) \qquad 1 \le i \le L \tag{19}$$

Experimentally, μ was varied from 0 to 25, and $\mu = 2$ was found to be ideal. The gain matrix $\boldsymbol{G}$ is obtained by diagonalizing the gain vector $\boldsymbol{q}$.
Step 7: Determine the linear KLTM estimator using (16).
Step 8: Estimate the KLTM-enhanced VEP signal using (17).

3. PERFORMANCE EVALUATION

The KLTM method was tested and assessed using artificial and real human data obtained from a hospital.

3.1 Assessment of the Algorithm using Artificial Data

The clean artificial VEP $\boldsymbol{x}$ is generated by superimposing several Gaussian functions; the amplitudes, variance and mean of these functions are tweaked to generate precise peak latencies at 100 ms, mimicking the real P100. The pre-stimulation EEG colored noise $\boldsymbol{e}(k)$ is generated using autoregressive (AR) model [5] given by the following equation.

$$\begin{aligned} \boldsymbol{e}(k) = 1.5084\boldsymbol{e}(k-1) - 0.1587\boldsymbol{e}(k-2) - \\ 0.3109\boldsymbol{e}(k-3) - 0.0510\boldsymbol{e}(k-4) + \boldsymbol{u}(k) \end{aligned} \tag{20}$$

where $\boldsymbol{u}(k)$ is the input driving noise of the AR filter and $\boldsymbol{e}(k)$ is the filter output. The artificial post-stimulation EEG noise $\boldsymbol{n}$ is generated by changing the variance of $\boldsymbol{e}$. Since noise is assumed to be additive, the artificially-corrupted VEP signal $\boldsymbol{y}$ is then produced by adding together $\boldsymbol{x}$ and $\boldsymbol{n}$.

To test the robustness of KLTM, the ratio of the artificial VEP over the EEG noise was varied from approximately +0 dB to -10 dB using the following formula:

$$\text{SNR (dB)} = 10\log\frac{\text{Power of VEP (Watts)}}{\text{Power of post-stimulus EEG (Watts)}} \tag{21}$$

The corrupted VEP signal with a specific value of SNR was applied to the input of the KLTM filter and the estimated P100 waveform was retrieved at the output. To obtain reliable statistics, five hundred different runs were performed for each level of SNR. Success rate, average errors, mean of peak latencies and standard deviations are used as performance indicators to assess the effectiveness of KLTM in single-trial estimation of VEP latencies. To measure success rate, visual inspections were performed to judge whether or not the estimators' processed waveforms are acceptable. The highest peak within 100 ±10 ms is considered as the wanted P100 component. Any trial is noted as a failure if the waveform fails to show clearly the pertinent peak within the stated ±10 ms tolerance. The success rate for each algorithm is expressed in terms of a percentage. It is calculated according to the following formula:

$$\text{success rate} = (\text{number of successes } / N) \times 100\% \tag{22}$$

where N is the number of runs (trials) per SNR which in this case equals to 500. Next, the average errors e_{P100} in estimating the latency of the P100 was calculated as follows:

$$e_{P100} = \sum_{i=1}^{500} \left| \hat{t}_{P100}(i) - 100 \right| \tag{23}$$

where $\hat{t}_{P100}(i)$ represents the estimated P100 latency in milliseconds. For five hundred runs per SNR, the average (mean) of the estimated P100 peak latencies, denoted as $\overline{P}_{100}$, is calculated as

$$\overline{P}_{100} = \sum_{i=1}^{500} \hat{t}_{P100}(i) \tag{24}$$

where $\hat{t}_{P100}(i)$ is the individually estimated latency of the P100 peak in milliseconds. Next, the standard deviation σ_{P100} of the P100 peak latencies is computed as

$$\sigma_{P100} = \sqrt{\sum_{i=1}^{500} (\hat{t}_{P100}(i) - \bar{t}_{P100})^2 / (500-1)} \tag{25}$$

where $\hat{t}_{P100}(i)$ and $\bar{t}_{P100}$ are the estimated P100 latencies and average value (in milliseconds), respectively, of the five hundred P100 data sets. Specifically, the P100 with a latency average closer to 100 ms, coupled with a narrower standard deviation indicate better performance.

Table 1 below tabulates the success rate, average errors, peak latency mean, and standard deviations for the KLTM estimator.

Table 1 - The success rate, average errors, peak latency mean and standard deviations of the KLTM estimator at SNR = 0 to -10 dB.

SNR [dB]	Success Rate [%]	Average Error	Mean Latency	Standard Deviation
0	98.7	4.1	101.2	2.6
-2	96.9	4.9	101.8	5.7
-4	94.3	5.1	102.4	5.9
-6	92.1	5.8	102.9	6.4
-8	89.6	6.7	103.5	7.5
-10	85.4	7.6	104.3	8.1

From Table 1, it can be stated that KLTM produces the highest success rate at 0 dB and the least success rate at -10 dB. Correspondingly, the lowest average error occurs at 0 dB and the highest one is generated at -10 dB also. The mean latency and standard deviation produced by KLTM increase slightly as the SNR value gets lower.

For some graphical illustrations, various waveforms with successfully estimated P100's at -6 and -10 dB are shown in Figure 1 below.

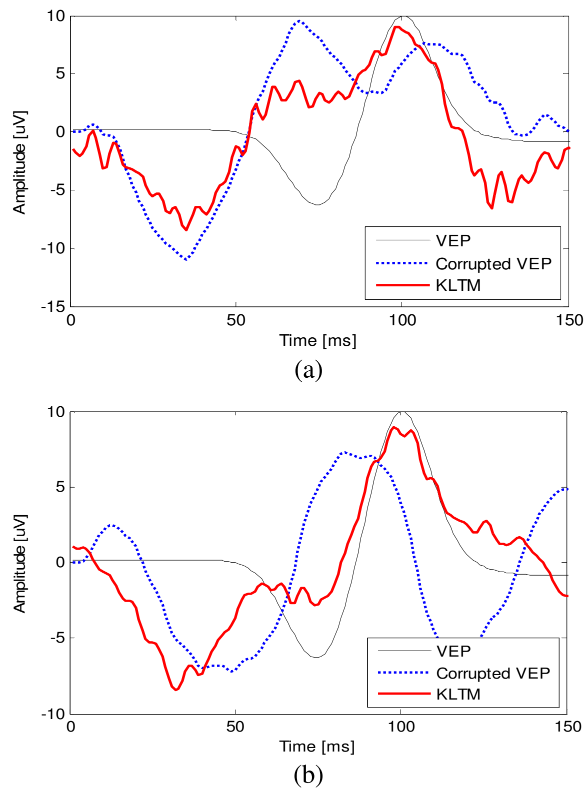

Figure 1 - Clean VEP, corrupted VEP, and estimated VEP waveforms by KLTM at (a) -6 dB; (b) -10 dB.

3.2 Assessment of the Algorithm using Human Data

This section evaluates KLTM in estimating human P100 peaks, which are used by doctors as objective evaluation of the visual pathway conduction. Experiments were conducted at Selayang Hospital, Kuala Lumpur using RETIport32 equipment, and carried out on sixteen subjects having **normal** (P100 ≤ 115 ms) and **abnormal** (P100 > 115 ms) VEP readings. They were asked to watch a pattern reversal checkerboard pattern. The detailed test setup (sampling frequency, electrode connections, etc.) can be found in [4, 6]. Eighty trials for each subject's right eye were processed by the VEP machine using ensemble averaging (EA). The averaged values were readily available and directly obtained from the equipment. Since EA is a multi-trial scheme, it is expected to produce good estimation of the P100 that can be used as a baseline for comparing the KLTM estimator performance.

Further, KLTM requires unprocessed data from the machine. Thus, the equipment was configured accordingly to generate the raw data. The recording for every trial involved capturing the brain activities for 333 ms before stimulation was applied; this enabled us to capture the colored EEG noise alone. The next 333 ms was used to record the post-stimulus EEG, comprising a mixture of the VEP and EEG. The same process was repeated for the consecutive trials. For comparisons with EA, the eighty different waveforms per subject produced by KLTM were also averaged. Again, the strategy here was to look for the highest peak from the averaged waveform. The purpose of averaging the outcome of KLTM was to establish the performance of KLTM as a single-trial estimator; the mean KLTM peak that is close to the EA peak reflects the accuracy of the individual single-trial outcome.

Illustrated in Figures 2(a) and 2(b) below are the KLTM's extracted Pattern VEPs for S1 from trial # 46 and for S7 from trial # 21, respectively. It is to be noted that any peaks that occur below 90 ms are noise and are therefore ignored. Attention is given to any dominant (i.e., highest) peak(s) from 90 to 140 ms.

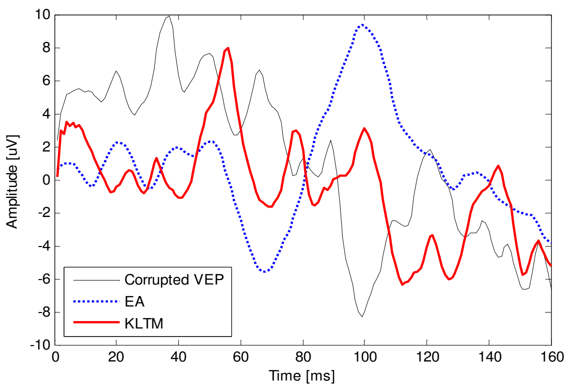

(a)

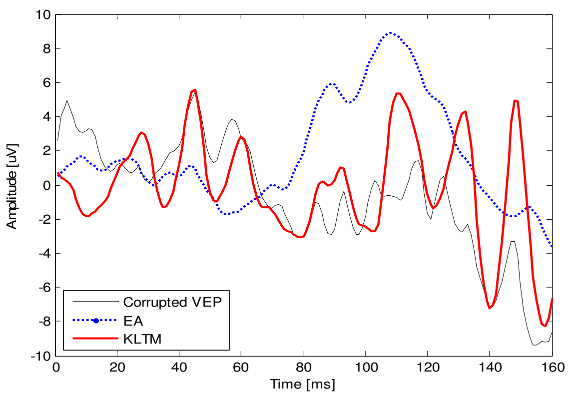

(b)

Figure 2 - The P100 of (a) the first subject (S1) taken from trial # 46; (b) the seventh subject (S7) taken from trial # 21.

From Figure 2(a), the highest peak produced by KLTM is at 100 ms, which is close to 99 ms obtained by EA. On the other hand, the corrupted VEP (unprocessed raw signal) contains a dominant peak at 121 ms. From Figure 2(b), the highest peak produced by KLTM is at 111 ms, which is close to 108 ms obtained by EA. However, the corrupted VEP shows a dominant peak at 117 ms.

Table 2 below summarizes the mean latency values of the P100's by EA and KLTM for the sixteen subjects, S1 to S16. If the maximum allowable mean error (e_m) is set at ±5, KLTM successfully estimated the P100's from twelve subjects: S1, S2, S3, S4, S6, S7, S8, S12, S13, S14, S15, and S16. On the other hand, KLTM unsuccessfully estimated the intended peaks from subjects S5, S9, S10, and S11. Therefore with the given number of subjects, the success rate for KLTM is at 75 %, and the average mean error is 4.5. In brief, the simulated and real data experiments exhibit the capability of KLTM in VEP estimation.

Table 2 - The mean latencies of P100's of the EA and KLTM estimators for sixteen different subjects.

Subject	EA Method	KLTM Method	Mean Error	Subject	EA Method	KLTM Method	Mean Error
S1	99	99	0	S9	130	145	15
S2	100	100	0	S10	117	108	9
S3	119	119	0	S11	119	111	8
S4	128	131	3	S12	114	113	1
S5	99	118	19	S13	102	103	1
S6	107	105	2	S14	123	118	5
S7	108	109	1	S15	102	105	3
S8	107	112	5	S16	108	108	0

4. CONCLUSION

A Karhunen Loeve transform method (KLTM) based on the eigendecomposition of the explicitly pre-whitened VEP signal covariance matrix has been presented and tested to estimate the VEP's P100 peaks severely degraded by colored EEG noise. The results of the simulated and real patient data reveal that the method is a promising technique that can be further refined and applied in the real world as a single trial estimator of biomedical signals, which are currently extracted by means of multi-trial ensemble averaging.

ACKNOWLEDGMENT

We would like to thank Dr. Tara Mary George and Mr. Mohd Zawawi Zakaria of the Ophthalmology Department, Selayang Hospital, Kuala Lumpur for the VEP data.

REFERENCES

[1] Y. Ephraim and H. L. Van Trees, “A Signal Subspace Approach for Speech Enhancement,” IEEE Transaction on Speech and Audio Processing, vol. 3, no. 4, pp. 251-266, July 1995.

[2] A. Rezayee and S. Gazor, “An Adaptive KLT Approach for Speech Enhancement,” IEEE Transactions on Speech and Audio Processing, vol.9, no.2, pp. 87-95, Feb. 2001.

[3] H. Lev-Ari and Y. Ephraim, "Extension of the Signal Subspace Speech Enhancement Approach to Colored Noise," IEEE Signal Processing Letters, vol. 10, no. 4, pp. 104-106, April 2003.

[4] M. Zuki Yusoff and N. Kamel, "Estimation of Visual Evoked Potentials for Measurement of Optical Pathway Conduction," in *Proc. 17th European Signal Processing Conference, 2009 (EUSIPCO 2009)*, Glasgow, Scotland, August 24-28, 2009, pp. 2322-2326.

[5] X. H. Yu, Z. Y. He and Y. S. Zhang, “Time-Varying Adaptive Filters for Evoked Potential Estimation,” IEEE Transactions on Biomedical Engineering, vol. 41, no. 11, pp. 1062-1071, Nov. 1994.

[6] N. Kamel and M. Zuki Yusoff, "A Generalized Subspace Approach for Estimating Visual Evoked Potentials," in *Proc. IEEE EMBC'08,* Vancouver, Canada, Aug. 20-24, 2008, pp. 5208-5211.